

# Breakup Reactions of Neutron Halo Nuclei

T. Nakamura

*Department of Physics, Tokyo Institute of Technology,  
2-12-1 O-Okayama, Meguro, Tokyo 152-8551, Japan.*

Recibido el 31 de enero de 2005; aceptado el 9 de marzo de 2005

We present experimental studies of breakup reactions of one-neutron halo nucleus  $^{11}\text{Be}$  and two-neutron halo nucleus  $^{11}\text{Li}$  with carbon and lead targets at approximately 70 MeV/nucleon at RIKEN. In the Coulomb breakup of  $^{11}\text{Be}$ , the selection of forward scattering angles has been found useful to extract the first-order E1 Coulomb breakup component, and to exclude the nuclear contribution and higher-order Coulomb breakup components. This angle-selected energy spectrum is thus used to deduce the spectroscopic factor for the halo configuration in  $^{11}\text{Be}$ , which has been found to be  $0.72 \pm 0.04$ . In the breakup of  $^{11}\text{Be}$  with the carbon target, we have observed excitations to the discrete states at  $E_x = 1.78$  MeV and  $E_x = 3.41$  MeV. Angular distributions for these states show the diffraction pattern characteristic of  $L = 2$  transitions. In the Coulomb breakup of  $^{11}\text{Li}$  we have observed the strong E1 excitation at  $E_{\text{rel}} \sim 300$  keV, which is very different from the previous observations. The non-energy weighted sum of E1 strength indicates the strong neutron-neutron correlations in  $^{11}\text{Li}$ .

**Keywords:** Spectroscopic factor; spin; parity; isobaric spin.

En este trabajo se presentan estudios experimentales realizados en RIKEN para las reacciones de desintegración del núcleo con un neutron en halo  $^{11}\text{Be}$  y con dos neutrones en halo  $^{11}\text{Li}$  con blancos de carbono y plomo a 70 Mev/nucleon, aproximadamente. Los ángulos de dispersión en la desintegración de Coulomb del  $^{11}\text{Be}$  con blanco de carbono han sido encontrados de gran utilidad para extraer el componente E1 de primer orden de desintegración de coulomb, así como excluir la contribución nuclear y las componentes de desintegración de coulomb de orden superior. Este espectro energético con selección de ángulo es usado para deducir los factores espectroscópicos para la configuración de halo del  $^{11}\text{Be}$ , el que ha sido encontrado  $0.72 \pm 0.04$ . En la desintegración del  $^{11}\text{Be}$  con blanco de carbono, observamos excitaciones a los estados discretos que se encuentran a energías  $E_x = 1.78$  MeV y  $3.41$  MeV. Las distribuciones angulares para esos estados muestran el patrón de difracción característico de las transiciones  $L = 2$ . En la desintegración de coulomb del  $^{11}\text{Li}$ , hemos observado una fuerte excitación E1 a  $E_{\text{rel}} \sim 300$  kev, la cual es muy diferente a la encontrada en experimentos anteriores. La suma de intensidades E1 indica una fuerte correlación neutron-neutron en  $^{11}\text{Li}$ .

**Descriptores:** Factor espectroscópico; espín; paridad; espín isobarico.

PACS: P21.10.Jx; 21.10.Hw; 24.50.+g

## 1. Introduction

Breakup reactions have played important roles in investigating the properties of halo nuclei, where both Coulomb and nuclear breakup cross sections are substantially enhanced compared to the ordinary nuclei. In this presentation, we characterize the breakup reactions of halo nuclei by showing the experimental results of 1) Coulomb breakup of the one-neutron halo nucleus  $^{11}\text{Be}$ , 2) nuclear breakup of the one-neutron halo nucleus  $^{11}\text{Be}$ , and 3) Coulomb breakup of the two-neutron halo nucleus  $^{11}\text{Li}$ .

Since most of the properties can be studied more clearly for a simple one-neutron halo nucleus, we have primarily studied  $^{11}\text{Be}$ . The  $^{11}\text{Be}$  nucleus is, in particular, suitable for investigating the reaction mechanisms since the ground state properties have been well investigated. For example, the one-neutron separation energy  $S_n$  is precisely known to be  $504 \pm 6$  keV [1].

The situation for two-neutron halo nuclei is more controversial. The previous three experiments on the Coulomb dissociation of  $^{11}\text{Li}$  [2–4] have been inconsistent with each other. It may be due to the fact that it is difficult to detect two neutrons unambiguously. Theoretically, reaction mechanisms suffer from the complexity which may arise from the two-neutron halo correlations. We have thus studied this case with much more statistics and with careful two-neutron detection.

We organize this paper according to the three breakup studies. Section 2. describes the breakup experiment of  $^{11}\text{Be}$  on a Pb target, which is dominated by the Coulomb breakup. Section 3. describe the breakup experiment of  $^{11}\text{Be}$  on a C target, which is dominated by the nuclear breakup. The details of these two experiments have been described in Ref. [5]. In Sec. 4. we present the preliminary results on the breakup of  $^{11}\text{Li}$  on a Pb target. Then, in Sec. 5., the conclusions are given.

## 2. Coulomb breakup of one-neutron halo nuclei – Case of $^{11}\text{Be}$

### 2.1. Coulomb breakup

Coulomb breakup (dissociation) has been a useful spectroscopic tool for loosely bound nuclei. Coulomb breakup can be described as a process in which the projectile passes a high- $Z$  target, is excited by absorption of a virtual photon from the changing target Coulomb field, and decays into a breakup channel involving a few particles. The advantage of this reaction is that the dissociation energy spectrum can be directly related to the electromagnetic transition matrix element  $B(E\lambda)$  which contains information on the structure of the projectile ground state [6, 7]. In the case of E1 excitation, the energy spectrum of Coulomb dissociation ( $d\sigma_{\text{CD}}/dE_x$ ) is

related to  $B(\text{E1})$  as in,

$$\frac{d\sigma_{\text{CD}}}{dE_x} = \int_{b_0}^{\infty} 2\pi b db \frac{N_{\text{E1}}(E_x, b)}{E_x} \sigma_{\gamma}^{\text{E1}}(E_x) \quad (1)$$

$$\frac{dB(\text{E1})}{dE_x} = \frac{9\hbar c}{16\pi^3} \frac{\sigma_{\gamma}^{\text{E1}}(E_x)}{E_x}, \quad (2)$$

where  $N_{\text{E1}}(E_x, b)$  is the number of virtual photons with energy  $E_x$  in a collision at impact parameter  $b$ , while  $\sigma_{\gamma}^{\text{E1}}(E_x)$  represents the E1 photo-absorption cross section at  $E_x$ . It is noted that this formula can be extracted by a semi-classical perturbation theory (Equivalent photon method). Below, we also show quantum mechanical calculations based on DWBA (ECIS code [8]) for an E1 excitation. These two methods provide almost identical excitation energy spectrum.

## 2.2. Large low-lying E1 excitation and direct breakup mechanism

In the Coulomb breakup of halo nuclei, it has now been well-established that the strong E1 excitation appears at low excitation energies for halo nuclei. Our previous  $^{11}\text{Be}$  experiment showed that the strong low-lying excitation can be explained by a so-called direct breakup mechanism [9, 10], where the halo nucleus breaks up instantly without forming any resonances. In the direct breakup mechanism, the  $B(\text{E1})$  distribution as a function of  $E_{\text{rel}} (= E_x - S_n)$  is described simply by the following matrix element,

$$\frac{dB(\text{E1})}{dE_{\text{rel}}} = |\langle \mathbf{q} | \frac{Ze}{A} r Y_m^1 | \Phi(\mathbf{r}) \rangle|^2. \quad (3)$$

$\Phi(\mathbf{r})$  stands for the wave function for  $^{11}\text{Be}$  in the ground state. The E1 operator involves  $r$ , the relative distance between the core and valence neutron. The final state  $\langle \mathbf{q} |$  describes a neutron in the continuum with relative momentum  $\mathbf{q}$ . We find that the matrix element represents approximately a Fourier transform of  $rR(r)$ . Thus in the case of halo nuclei, whose radial wave function has large amplitude at large  $r$ , the  $B(\text{E1})$  spectrum has a peak at low relative energy (corresponding to small  $\mathbf{q}$ ).

This fact enables the Coulomb breakup to be a useful spectroscopic tool. Since the amplitude of  $B(\text{E1})$  reflects that of  $\Phi(\mathbf{r})$  at large distance, the normalization of  $B(\text{E1})$  provides the spectroscopic factor for the halo configuration in the ground state. In the case of  $^{11}\text{Be}$ , where the wave function can be decomposed as in,

$$|^{11}\text{Be}(1/2^+) \rangle = \alpha |^{10}\text{Be}(0^+) \otimes \nu 2s_{1/2} \rangle + \beta |^{10}\text{Be}(2^+) \otimes \nu 1d_{5/2} \rangle + \dots, \quad (4)$$

Since the first term represents the halo configuration due to no centrifugal barrier for the  $s$ -wave neutron, the amplitude of  $B(\text{E1})$  can be used to extract  $\alpha^2$ . From the previous work we extracted  $\alpha^2$  to be  $0.8 \pm 0.2$ , while the recent experiment at 520 MeV/nucleon at GSI gave the value of  $0.61 \pm 0.05$  [11].

This spectroscopic method has been applied to the other cases, such as neutron rich  $^{15}\text{C}$ ,  $^{17}\text{C}$  [12, 13], and  $^{19}\text{C}$  [14]. For instance, the halo structure has been clearly shown for the case of  $^{19}\text{C}$  where dominant halo configuration with  $s$ -wave neutron was observed [14].

## 2.3. Remaining issues

Although the Coulomb dissociation has successfully been used as a spectroscopic tool for halo nuclei, there remain some open questions for more precise evaluation of the spectroscopic factor. We categorize such problems into the following three issues: 1) Higher order Coulomb breakup effects [15–21], 2) Larger nuclear breakup contaminants [20–23], and 3) The choice of final state interactions.

In order to disentangle these problems, we revisited the Coulomb breakup of  $^{11}\text{Be}$  with much higher statistics. In this new experiment, we focused on extracting the information of the scattering angle  $\theta$  of  $^{10}\text{Be} + \text{n}$  c.m. system. The angle  $\theta$  is related to the impact parameter  $b$  by  $b = a \cot(\theta/2) \simeq 2a/\theta$  for the semi-classical Coulomb breakup trajectory. One can then select safely the region of almost pure E1 Coulomb breakup by using the information of  $\theta$ , and can exclude higher order Coulomb breakup contributions and nuclear breakup contaminants.

In the experiment, we measure the momentum vector of incident  $^{11}\text{Be}$  ( $\mathbf{P}^{(11)\text{Be}}$ ) as well as the momentum vectors of outgoing  $^{10}\text{Be}$  ( $\mathbf{P}^{(10)\text{Be}}$ ) and neutron ( $\mathbf{P}(\text{n})$ ) in coincidence. The angle  $\theta$  can be determined by the opening angle between the direction of  $\mathbf{P}^{(11)\text{Be}}$  and that of the outgoing vector of the center of mass obtained by  $\mathbf{P}^{(10)\text{Be}} + \mathbf{P}(\text{n})$ . The excitation energy  $E_x$  or relative energy  $E_{\text{rel}}$  ( $E_{\text{rel}} = E_x - S_n$ ) can be obtained by reconstructing the invariant mass of the intermediate excited state of  $^{11}\text{Be}$ . The invariant mass is a function of  $\mathbf{P}^{(10)\text{Be}}$  and  $\mathbf{P}(\text{n})$ . The detail of the experimental apparatus to measure the momentum vectors is described in Ref. [5].

## 2.4. Results of $^{11}\text{Be}$ Coulomb breakup

Figure 1 shows the angular distribution of  $^{10}\text{Be} + \text{n}$  center of mass system in the  $^{11}\text{Be}$  breakup on the Pb target. It is seen that the angular distribution is characterized by a forward peak. The most forward part can be well explained by the pure E1 Coulomb breakup calculation shown by a solid curve, where the ECIS code is used. However, it should be noted that a small deviation is seen at larger angles. In the figure, we also show the impact parameter axis on the top as a reference. We can see that the agreement is perfect for the impact parameter over 30 fm, which is equivalent to  $\theta \leq 1.3$  degrees. Such selection can then be used to extract the pure E1 Coulomb breakup component.

Figure 2 shows the relative energy spectrum for the whole angular acceptance and that for the selected forward angles ( $\theta \leq 1.3^\circ$ ). It is clearly seen that the spectrum selected for the forward angles is perfectly in agreement with the pure

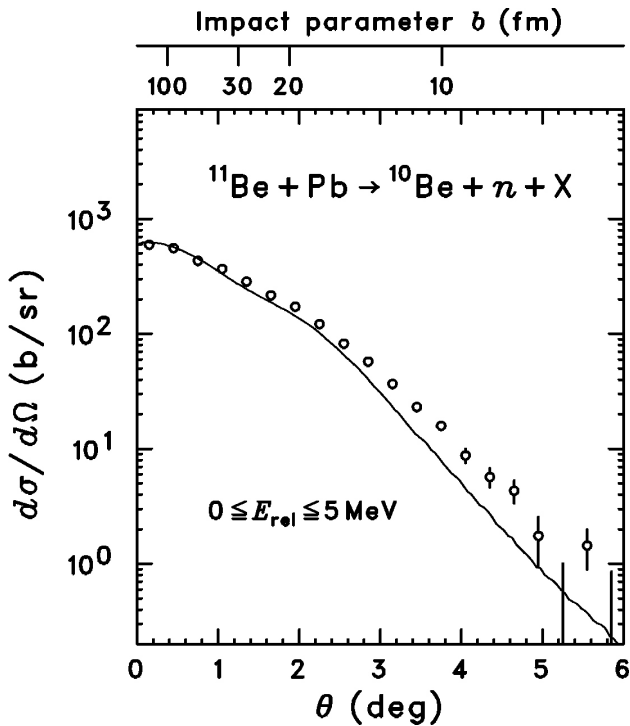


FIGURE 1. Angular distribution of the  $^{10}\text{Be} + n$  c.m. system scattered by the Pb target for the  $E_{\text{rel}}$  ranges of  $0 \leq E_{\text{rel}} \leq 5$  MeV. The solid curve shows the calculated results with the ECIS code for a pure E1 breakup.

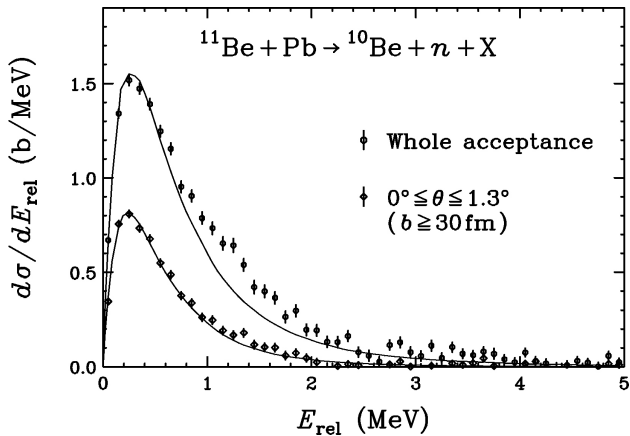


FIGURE 2. Relative energy spectrum of  $^{11}\text{Be}$  on the Pb target at 69 MeV/nucleon for the whole acceptance (open circles), and for the selected forward angles less than 1.3 degrees (open diamonds). The solid curve is the calculation for the E1 direct breakup model (pure Coulomb). It is seen that the angle-selected data is in perfect agreement with the calculation.

E1 direct breakup calculation shown by the solid curve. This result confirms that the pure E1 breakup is, in fact, selected and that the higher-order Coulomb breakup component and nuclear breakup contribution is almost excluded for the spectrum for the forward angles. By using this selected data, one could also extract the spectroscopic factor for the halo configuration to be  $0.72 \pm 0.04$ , which is more precise than the previously known values.

With the same  $\alpha^2$  value, we can calculate also the whole angular range. An overall agreement with the data is obtained although the small deviation is seen around  $E_{\text{rel}}=1\text{--}2$  MeV. This may due to the effect of higher order Coulomb breakup and nuclear breakup contribution. The comparison with these effects is described in Ref. [5].

### 3. Nuclear breakup of one-neutron halo nuclei—Case of $^{11}\text{Be}$

For investigating the nuclear breakup, we have used a  $^{12}\text{C}$  target, where small  $Z$  allows much smaller Coulomb breakup contribution. Here, we focus on investigating the excitation of discrete states above the neutron breakup threshold by using the information of the excitation energy spectrum in combination with the scattering angle. We aim at establishing a spectroscopic method to study the narrow discrete states in the continuum. Such states are hardly observed in the breakup with a heavy target due to the large direct-breakup contribution. Since  $^{12}\text{C}$  is a iso-scalar target, we expect that the positive parity states can be populated.

Figure 3 shows the relative energy spectrum for the  $^{11}\text{Be} + \text{C}$  reaction. We notice that the spectrum is very different from the one for the Pb target described in the previous section. We have observed two discrete peaks in the relative energy spectrum, which are assigned to the known states at  $E_x=1.78$  MeV and 3.41 MeV. We have extracted the angular distributions of these states by subtracting properly the continuum, whose results are shown in Fig. 4. The data are compared to ECIS calculations with two appropriate optical potentials. We have found that these two peaks have  $L=2$  properties. The  $J^\pi$  for 1.78 MeV and 3.41 MeV states are thus assigned most probably  $5/2^+$  and  $3/2^+$ , respectively, as expected from the shell model calculation.

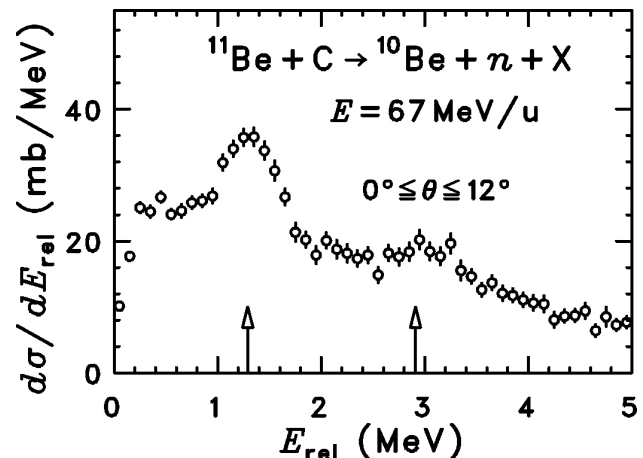


FIGURE 3. Relative energy spectrum in the  $^{11}\text{Be} + \text{C}$  reaction. The two arrows show  $E_x=1.78$  MeV and 3.41 MeV states, respectively. Note that  $E_{\text{rel}}=E_x - S_n$  with the one neutron separation energy  $S_n=504$  keV. Right: Known energy levels of  $^{11}\text{Be}$  [1, 24].

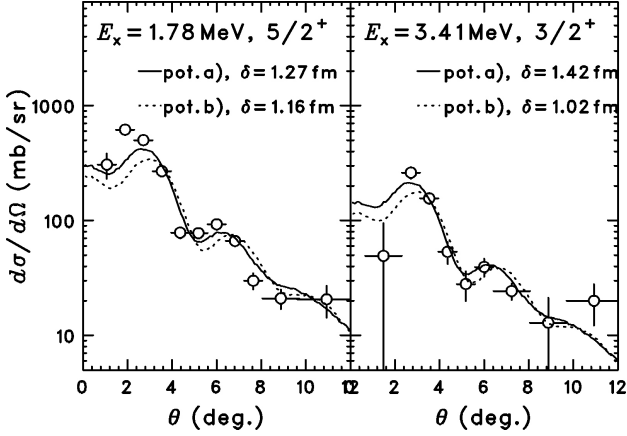


FIGURE 4. Angular distributions of the  $^{10}\text{Be} + \text{n}$  center of mass system corresponding to the 1.78 MeV(left) and 3.41 MeV(right) states. The comparison with the ECIS calculations with two optical potentials (written as a) and b)) shows that both angular distributions have  $L=2$  characteristics. The detail of the potential parameters is described in Ref. [5].

#### 4. Coulomb breakup of two-neutron halo nuclei – Case of $^{11}\text{Li}$

In the previous sections, we have seen that breakup of one-neutron halo nucleus can be well understood. On the contrary, the situation for the two neutron halo nuclei is complicated due to two neutron correlations. In the case of Coulomb breakup of  $^{11}\text{Li}$ , which is a typical two neutron halo nucleus with  $S_{2n} = 300 \pm 19$  keV [1], there have been three experiments done at MSU [2], RIKEN [3], and GSI [4], whose resultant  $B(E1)$  distributions are inconsistent with each other as shown in Fig. 5(right).

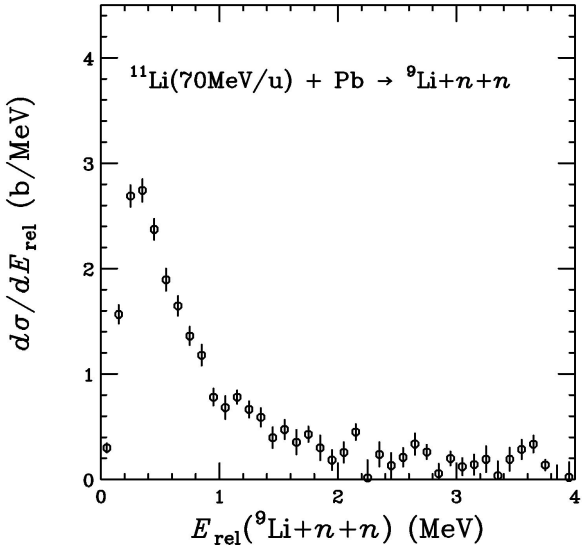


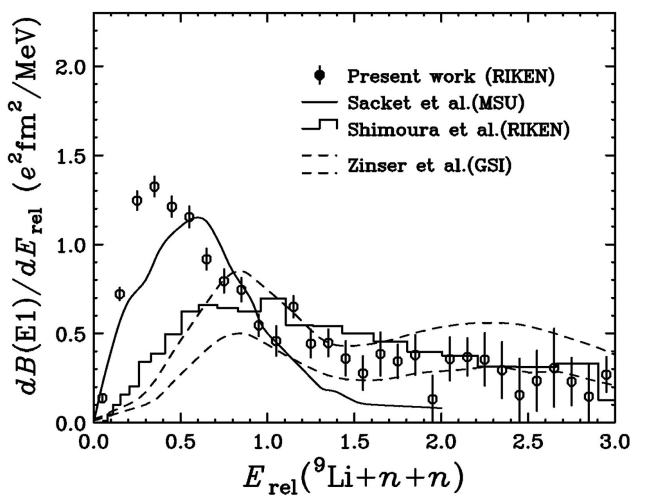
FIGURE 5. Left: Relative energy spectrum of three body breakup ( $^{9}\text{Li} + \text{n} + \text{N}$ ) of  $^{11}\text{Li}$  on Pb target. Right: The obtained  $B(E1)$  distribution (preliminary) is plotted by circles. The present result is compared with MSU result (solid), GSI result (zone between dashed curve), and RIKEN result (histogram). The new result shows a strong peak at lower relative energies.

#### 4.1. Coulomb breakup experiment on $^{11}\text{Li}$

We have thus studied the Coulomb dissociation of  $^{11}\text{Li}$  on a Pb target at an incident energy of approximately 70 MeV/nucleon to obtain the data with much higher statistics and much less ambiguity caused by crosstalk events in detecting two neutrons. A secondary beam of  $^{11}\text{Li}$  was produced by fragmentation of a 100 MeV/nucleon primary  $^{18}\text{O}$  beam in a thick Be production target and separated using the RIPS radioactive beam line at RIKEN. The  $^{11}\text{Li}$  beam bombarded a Pb target of thickness  $346 \text{ mg/cm}^2$  with an average energy of 70 MeV/nucleon. The momentum of the beam ion was obtained by tracing the trajectory with two PPAC's and by measuring the time of flight (TOF) using a thin plastic scintillator and an RF signal. The outgoing particles, a  $^{9}\text{Li}$  ion and two neutrons, were emitted in a narrow kinematical cone at forward angles. The trajectory of the  $^{9}\text{Li}$  ion was bent using a large-gap dipole magnet, tracked with a drift chamber, and then the  $^{9}\text{Li}$  ion hit a hodoscope. The momentum of the  $^{9}\text{Li}$  ion was thus obtained using the tracking information in combination with the TOF. The momentum of neutrons was obtained using the TOF and position information at the neutron detector arrays, which were composed of 54 rods of plastic scintillators arranged into two layers. Two layer arrangement is used to disentangle the cross talk events by selecting a kinematical condition. The momentum vectors of outgoing three particles were then combined to extract the invariant mass of the excited  $^{11}\text{Li}$  nuclei.

#### 4.2. Preliminary results of Coulomb breakup of $^{11}\text{Li}$

Figure 5 shows the preliminary spectrum of the relative energy of the three outgoing particles,  $^{9}\text{Li}$  and two neutrons in the breakup of  $^{11}\text{Li}$  on Pb. In the energy spectrum of dissoci-



ation (left), a large peak at  $E_{\text{rel}} \sim 0.3$  MeV is observed. The cross section amounts to  $2.35 \pm 0.05(\text{stat.})$  barns for  $E_{\text{rel}} \leq 3$  MeV and  $0 \leq 5$  degrees (preliminary). By using the equivalent photon method,  $B(E1)$  distribution was then obtained, whose result is shown in Fig. 5 (right). The new result shows the lower energy peak around 300 keV compared to the previous three experiments which peaked around 600–1000 keV. This substantial difference may be due to the insensitivity at low relative energies in the previous three experiments. The observed  $B(E1)$  spectrum peaked at lower excitation energies with higher strengths is rather consistent with a model incorporating strong two neutron correlations [25]. One can also examine such correlations by using the non-energy weighted E1 sum rule written by,

$$\begin{aligned} B(E1) &= \int_0^{+\infty} \frac{dB(E1)}{dE_{\text{rel}}} dE_{\text{rel}} \\ &= \frac{3}{4\pi} \left( \frac{Ze}{A} \right)^2 \langle r_1^2 + r_2^2 + 2\mathbf{r}_1 \cdot \mathbf{r}_2 \rangle, \end{aligned} \quad (5)$$

where  $r_1, r_2$  are the coordinates of two valence neutrons relative to the core. The term  $\mathbf{r}_1 \cdot \mathbf{r}_2$  contains the opening angle of two valence neutrons, which is a measure of two neutron correlations. The integrated  $B(E1)$  strength obtained in the current experiment is  $1.5 \pm 0.1$  e<sup>2</sup>fm<sup>2</sup>. By incorporating the value  $\sqrt{\langle r^2 \rangle}$  of about 5.1 fm [3], the average opening angle between two neutrons relative to the core becomes about 60 degrees, which is smaller than the independent two neutron model which has an average opening angle of 90 degrees. Further detailed analysis on two neutron correlation as well as n-<sup>9</sup>Li correlation is still in progress.

## 5. Conclusions

We have studied Coulomb and nuclear breakup of the one neutron halo nucleus <sup>11</sup>Be with high statistics. For the

breakup with the lead target, we have shown that the higher order effects and the nuclear breakup contaminants are very small and are well controlled by incorporating the analysis of the scattering angle of <sup>10</sup>Be + neutron. The spectroscopic amplitude for the halo states was thus extracted precisely. We have then shown the <sup>11</sup>Be + C breakup data for studying the discrete states above the neutron-decay threshold. There, we have observed the excitation to the known discrete state at  $E_x=1.78$  MeV and 3.41 MeV. The angular distribution for these states show  $L=2$  characteristics.

Finally, we have shown preliminary spectra for the new Coulomb breakup experiment on <sup>11</sup>Li. We have observed strong  $B(E1)$  peak at about  $E_{\text{rel}}=300$  keV, which is significantly different from the previous three experiments. The strong  $B(E1)$  can be interpreted as a revelation of strong n-n correlation in <sup>11</sup>Li. Further evidence is now being investigated by detailed analysis.

## Acknowledgement

The experiments on <sup>11</sup>Be have been done in collaboration with N. Fukuda, T. Kobayashi, H. Otsu, N. Aoi, H. Iwasaki, M. Notani, H. Sakurai, S. Shimoura, T. Teranishi, Y.X. Watanabe, K. Yoneda, T. Kubo, A. Mengoni, Y. Yanagisawa, N. Imai, and M. Ishihara. The experiments on <sup>11</sup>Li have been done in collaboration with A.M. Vinodkumar, T. Sugimoto, N. Fukuda, M. Miura, Y. Kondo, N. Aoi, N. Imai, T. Kubo, T. Kobayashi, T. Gomi, A. Saito, H. Sakurai, S. Shimoura, D. Bazin, H. Hasegawa, H. Baba, T. Motobayashi, K. Watanabe, Y.X. Watanabe, T. Yakushiji, Y. Yanagisawa, K. Yoneda, and M. Ishihara. The present work was supported in part by a Grant-in-Aid for Scientific Research (No.15540257) from the Ministry of Education, Culture, Sports, Science and Technology (MEXT, Japan).

---

1. A.H. Wapstra, G. Audi, and C. Thibault, *Nucl. Phys. A* **729** (2003) 129; G. Audi, A.H. Wapstra and C. Thibault, *Nucl. Phys. A* **729** (2003) 337, and references therein.
2. K. Ieki *et al.*, *Phys. Rev. Lett.* **70** (1993) 730 ; D. Sackett *et al.*, *Phys. Rev. C* **48** (1993) 118.
3. S. Shimoura *et al.*, *Phys. Lett. B* **348** (1995) 29.
4. M. Zinser *et al.*, *Nucl. Phys. A* **619** (1997) 151.
5. N. Fukuda, T. Nakamura *et al.*, *Phys. Rev. C* **70** (2004) 054606.
6. J.D. Jackson, *Classical Electrodynamics*, 2nd Edition (Wiley, New York 1975).
7. C. Bertulani and G. Baur, *Phys. Rep.* **163** (1988) 299.
8. J. Raynal, Coupled channel code ECIS97, also Notes on ECIS94, unpublished.
9. T. Nakamura *et al.*, *Phys. Lett. B* **331** (1994) 296.
10. A. Mengoni *et al.*, in *Proceedings of the International Symposium on Capture gamma-ray and Related topics*, edited by G.L. Molnar, T. Belgya and Zs. Revay, (Springer, 1997), p. 416.
11. R. Palit *et al.*, *Phys. Rev. C* **68** (2003) 034318.
12. U. Datta Pramanik *et al.*, *Phys. Lett. B* **551** (2003) 63.
13. T. Nakamura *et al.*, *Nucl. Phys. A* **722** (2003) 301c.
14. T. Nakamura *et al.*, *Phys. Rev. Lett.* **83** (1999) 1112.
15. G. Baur, C.A. Bertulani, and D.M. Kalassa, *Nucl. Phys. A* **550** (1992) 527.
16. T. Kido, K. Yabana, and Y. Suzuki, *Phys. Rev. C* **53** (1996) 2296.
17. V.S. Melezhik and D. Baye, *Phys. Rev. C* **59** (1999) 3232.
18. S. Typel and G. Baur, *Phys. Rev. C* **64** (2001) 024601.
19. S. Typel and R. Shyam, *Phys. Rev. C* **64** (2001) 024605.
20. J. Margueron, A. Bonaccorso, and D.M. Brink, *Nucl. Phys. A* **703** (2002) 105.

21. J. Margueron, A. Bonaccorso, and D.M. Brink, *Nucl. Phys. A* **720** (2003) 337.
22. C.H. Dasso, S.M. Lenzi, and A. Vitturi, *Phys. Rev. C* **59** (1999) 539.
23. M.A. Nagarajan, C.H. Dasso, S.M. Lenzi, and A. Vitturi, *Phys. Lett. B* **503** (2001) 65.
24. F. Ajzenberg-Selove, *Nucl. Phys. A* **506** (1990) 1.
25. H. Esbensen and G.F. Bertsch, *Nucl. Phys. A* **542** (1992) 310.